7

Contribution of Kuroshio Recirculation to Nutrient Transport Along the Kuroshio South of Japan: An Analysis of Model Results

Xinyu Guo[1,2], Yingying Hu[1], and Yoshikazu Sasai[2]

ABSTRACT

In this chapter, a brief review is given of an estimation of nutrient transport along the Kuroshio from east of Taiwan to south of Japan. Previous estimations were essentially based on observations that were limited in area and time. To understand downstream transport by the Kuroshio more broadly, we present a new estimation of nutrient transport using the results of an eddy-resolving nitrogen-based four-component nitrate–phytoplankton–zooplankton–detritus (NPZD) type model. Based on these calculations, we not only show the downstream nutrient transport along the Kuroshio path but also pay particular attention to the contribution of recirculation to nutrient transport increasing along the Kuroshio south of Japan as described in Guo et al. (2013) based on observation data along several sections of the Kuroshio. From the viewpoint of the entire Kuroshio south of Japan, recirculation of the Kuroshio contributes to nitrate transport only on the order of 45 kmol s^{-1}, which is much smaller than the previously reported value by one order. The previous estimation considered only the joining of recirculation into the Kuroshio but neglected the departure of recirculation from the Kuroshio.

7.1. INTRODUCTION

As the Kuroshio flows from low latitude to midlatitude regions, it carries not only heat but also many dissolved materials. Nutrients are one of the important materials with horizontal nitrate transport reported to be on the order of 100–200 kmol s^{-1} in the East China Sea (Chen et al., 1994, 1995, 2017; Guo et al., 2012, 2013) and, downstream, higher nitrate transport is reported to be on the order of 800–1300 kmol s^{-1} in the Kuroshio south of Japan. The joining of the Ryukyu Current into the Kuroshio south of Japan is partly responsible for this increase because the Ryukyu Current carries nitrate with horizontal transport on the order of 300 kmol s^{-1} (Guo et al., 2013). Another process is the joining of the Shikoku Basin local recirculation (Nagano et al., 2013) (hereafter called the Kuroshio recirculation) into the Kuroshio, which is estimated to make a large contribution to the downstream increase of horizontal nitrate transport within the Kuroshio between the two sections across the Kuroshio south of Japan.

The question is whether intensification of the downstream nitrate transport within the Kuroshio by the Kuroshio recirculation is applicable over the entire area of the Kuroshio south of Japan. In the case that the Kuroshio recirculation joins into the Kuroshio main stream, it acts to increase the horizontal nitrate transport within the Kuroshio. However, in the case that the Kuroshio recirculation departs from the Kuroshio main stream, such intensification is unlikely from the viewpoint of water budget.

Currently available estimations by Guo et al. (2013) are based on observations limited to the area west of 137°E. To clarify the contribution of the Kuroshio recirculation on downstream nitrate transport within the Kuroshio main stream, we use the results of a biogeochemical model that covers the entire area of the Kuroshio south

[1] *Center for Marine Environmental Studies, Ehime University, Ehime, Japan*

[2] *Japan Agency for Marine-Earth Science and Technology, Kanagawa, Japan*

Kuroshio Current: Physical, Biogeochemical, and Ecosystem Dynamics, Geophysical Monograph 243, First Edition.
Edited by Takeyoshi Nagai, Hiroaki Saito, Koji Suzuki, and Motomitsu Takahashi.

of Japan. The spatial change of horizontal nitrate transport through several sections across the Kuroshio with different locations relative to the Kuroshio recirculation suggests that the contribution of the Kuroshio recirculation to net downstream nitrate transport within the entire Kuroshio south of Japan is very limited.

We present model information and analysis method of model results in Section 7.2. The volume and nitrate transport through several sections are given in Section 7.3, and a discussion on the contribution of Kuroshio recirculation on the nitrate transport within the Kuroshio is given in Section 7.4, followed by a summary in Section 7.5.

7.2. MODEL AND MEAN CURRENT FIELD

We have used the Ocean general circulation model For the Earth Simulator (OFES) with sea-ice process (Masumoto et al., 2004; Komori et al., 2005; Sasaki et al., 2008) coupled to a simple nitrogen-based Nitrate–Phytoplankton–Zooplankton–Detritus (NPZD) pelagic model (Oschilies, 2001). Details of the biological model are described elsewhere (Sasai et al., 2006, 2010). The OFES domain extends from 20°S in the South Pacific to 66°N in the North Pacific Ocean and from 100°E to 70°W. The OFES is 1/10° horizontal resolution and has 54 vertical levels from 5 m thickness at the surface to 330 m thickness at the maximum depth of 6065 m. The OFES was integrated for 30 years under climatological forcing using the Japanese 25-year Reanalysis (JRA25) (Onogi et al., 2007), from the observed climatological fields of temperature and salinity fields (World Ocean Atlas, 2009 (WOA09)) (Locarnini et al., 2010; Antonov et al., 2010) without motion. After 30 years of spin-up integration, the OFES was forced by six-hourly JRA25 from 1979 to 1994. The last day of 1994 is used for the initial physical fields for this simulation.

To reach equilibrated biological fields, the biological model was incorporated after 30 years spin-up of the OFES with JRA25 climatological forcing. The biological model coupled with the evolving physical fields was integrated a further five-year period under the climatological forcing. The biological fields in the last year of the coupled five-year integration were used as initial conditions for this simulation. The coupled physical-biological model was forced by six-hourly JRA25 from 1995 to 2012. In this study, we used monthly mean of model results for nitrate, phytoplankton, detritus, zooplankton, and horizontal velocity covering 1995– 2012 from coupled physical-biological model.

In the analysis, we define the Kuroshio south of Japan as that from the Tokara Strait (section TN–TS, Figure 7.1a) to the Izu-Ogasawara Ridge (section IN–IS). For the surface current velocity averaged over 1995– 2012,

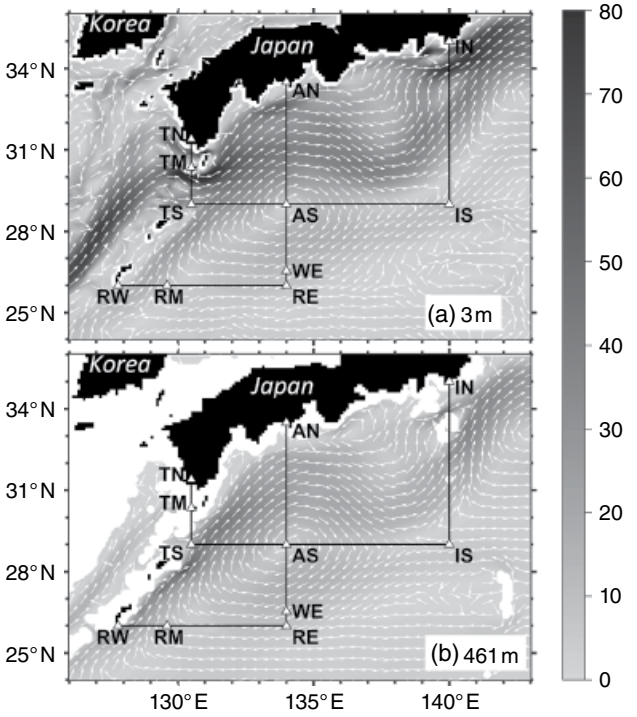

Figure 7.1 Map of study area and the horizontal distribution of mean currents (gray colors represent the magnitude of current velocity (cm s^{-1}) and arrows represent direction) at a depth of (a) 3 m and (b) 461 m. Land areas are shaded in black. We choose two zonal sections (RW–RM–RE and TS–AS–IS) and three meridional sections (TN–TM–TS, AN–AS–RE and IN–IS) for the calculation for volume and nitrate transports. Black triangles labeled with letters indicate endpoints of sections and points dividing the sections.

the Kuroshio west of the Tokara Strait shows a strong current (0.7–0.8 m s^{-1}) in the East China Sea (Figure 7.1a). In the Tokara Strait and the area east of the Izu-Ogasawara Ridge, the Kuroshio also shows a strong current with a mean velocity of over 0.8 m s^{-1}. However, the mean velocity of the Kuroshio between the Tokara Strait and the Izu-Ogasawara Ridge is relatively weak and broad, which is likely due to meandering of the Kuroshio path south of Japan.

An anticyclonic circulation with a center at point AS can be found in the surface mean current (Figure 7.1a). This anticyclonic circulation is the Kuroshio recirculation that joins the Kuroshio west of point AS and diverges from the Kuroshio east of point AS. A northeastward current from the offshore side of the Ryukyu Islands also joins the Kuroshio at the west edge of the anticyclonic circulation.

To separate the contribution of Kuroshio recirculation and the northeastward current from eastern side of the Ryukyu Islands to the Kuroshio south of Japan, we

designated several sections (Figure 7.1a) to estimate volume transport and nitrate transport in various compartments. The Kuroshio recirculation appears mainly as the westward current through section AS–RE and the southward current through section AS–IS. The northeastward current east of the Ryukyu Islands is approximated by the current through section RW–RM. Within the Kuroshio, flow through the Tokara Strait is represented by section TN–TM–TS; flow south of Japan by section AN–AS; and flow going to the Kuroshio Extension by section IN–IS.

As shown in Figure 7.1b, the mean current at the depth of 461 m weakens but maintains a similar structure to that in the surface layer (Figure 7.1a). Because of the consistent current structure in the vertical direction, we expect that these sections work well for the purpose of capturing different currents in the Kuroshio south of Japan.

7.3. RESULTS

7.3.1. Vertical Profile of Mean Current Velocity and Volume Transport Through Sections

Since nutrient flux depends closely on current velocity, we first examine the vertical structure of current velocity and then present transport through these sections. At the Tokara Strait, the eastward current (>0.1 m s^{-1}) is centered at layers shallower than 500 m at section TM–TS and at shallow areas of section TM–TN (Figure 7.2a). Moving downstream from the Tokara Strait, the eastward Kuroshio occupies most of section AN-AS with a significant current (0.3~0.4 m s^{-1}) at the surface. Meanwhile, the westward current (=Kuroshio recirculation) appears at section AS–RE with a velocity of over 0.1 m s^{-1} at the surface layer (Figure 7.2b). Moving farther downstream, the eastward current occupies most of section IN–IS, while the westward flowing recirculation of the Kuroshio is not observed at the section (Figure 7.2c).

At the two zonal sections (Figures 7.2d, 7.2e), we observe a similar current structure: a northward current is at the western side while a southward current is at the eastern side. The northward current has a subsurface maximum core that is weak at section RW–RM but strong at section TS–AS. The southward current has a surface maximum velocity that is weak at section RM–RE but strong at section AS–IS. The stronger northward and southward currents at section TS–IS than at section RW–RE reflect the presence and absence of Kuroshio recirculation at these two sections.

Volume transport through each grid point integrated from sea bottom to sea surface has apparent horizontal variation along the sections (Figure 7.3). At the Tokara Strait, eastward transport is concentrated at section TM–TS where total transport is 16.4 Sv while that through section TN–TM is 1.1 Sv. The largest eastward transport (74.1 Sv) is found at section AN–AS, where the transport is large at the center of the section and gradually decreases to zero to the north and south. The Kuroshio recirculation induces a westward transport through section AS–RE (37.7 Sv) and a southward transport through section AS–IS (33.0 Sv), both of which show relatively large values at the segment half close to point AS. Eastward transport through section IN–IS is 41.1 Sv with peaks around 34°N and 32°N. This value (41.1 Sv) reflects the difference between the eastward transport through section AN–AS and southward transport through section AS–IS.

The Kuroshio recirculation has little effect on section RW–RE, where northward transport concentrates at the western side between RW and RM. Therefore, northward transport through section RW–RE can be considered as a net contribution to the Kuroshio south of Japan. Actually, the combination of northward transport through section RW–RE and westward transport through section AS–RE nearly balances with the northward transport through section TS–AS (the exact balance needs an eastward volume transport of 1.1 Sv through section RW–TS that has been confirmed by a direct calculation of volume transport). The westward shift of the maximum northward transport along section TS–AS is likely caused by the joining of the northward current through section RW–RE. Therefore, eastward transport through section IN–IS is likely the true Kuroshio transport that comprises two components: one from the East China Sea and the other from the eastern side of the Ryukyu Islands. The Kuroshio recirculation acts as a local acceleration engine to the Kuroshio south of Japan.

The mean Kuroshio transport was estimated to be 42 Sv by Imawaki et al. (2001) by combining satellite altimeter with *in situ* hydrographic and current measurement data at a section south of Japan (ASUKA-line). In this estimation, the Kuroshio recirculation was defined as a westward current across the section and has a transport of 15 Sv. Sugimoto et al. (2010) reported a mean Kuroshio transport of 33 Sv for another section south of Japan (137°E) and a Kuroshio recirculation of 15.6 Sv there. Both the estimations given by Imawaki et al. (2001) and Sugimoto et al. (2010) were performed at a spatially fixed section and such method has a possibility not fully capturing the recirculation due to its variation in position. Nagano et al. (2013) gave a physically reasonable definition on the Kuroshio recirculation south of Japan by assuming its little contribution to the Kuroshio transport flowing into the Kuroshio extension area. Following their idea, we specified a point (WE) at section AS–RE by setting the westward transport through

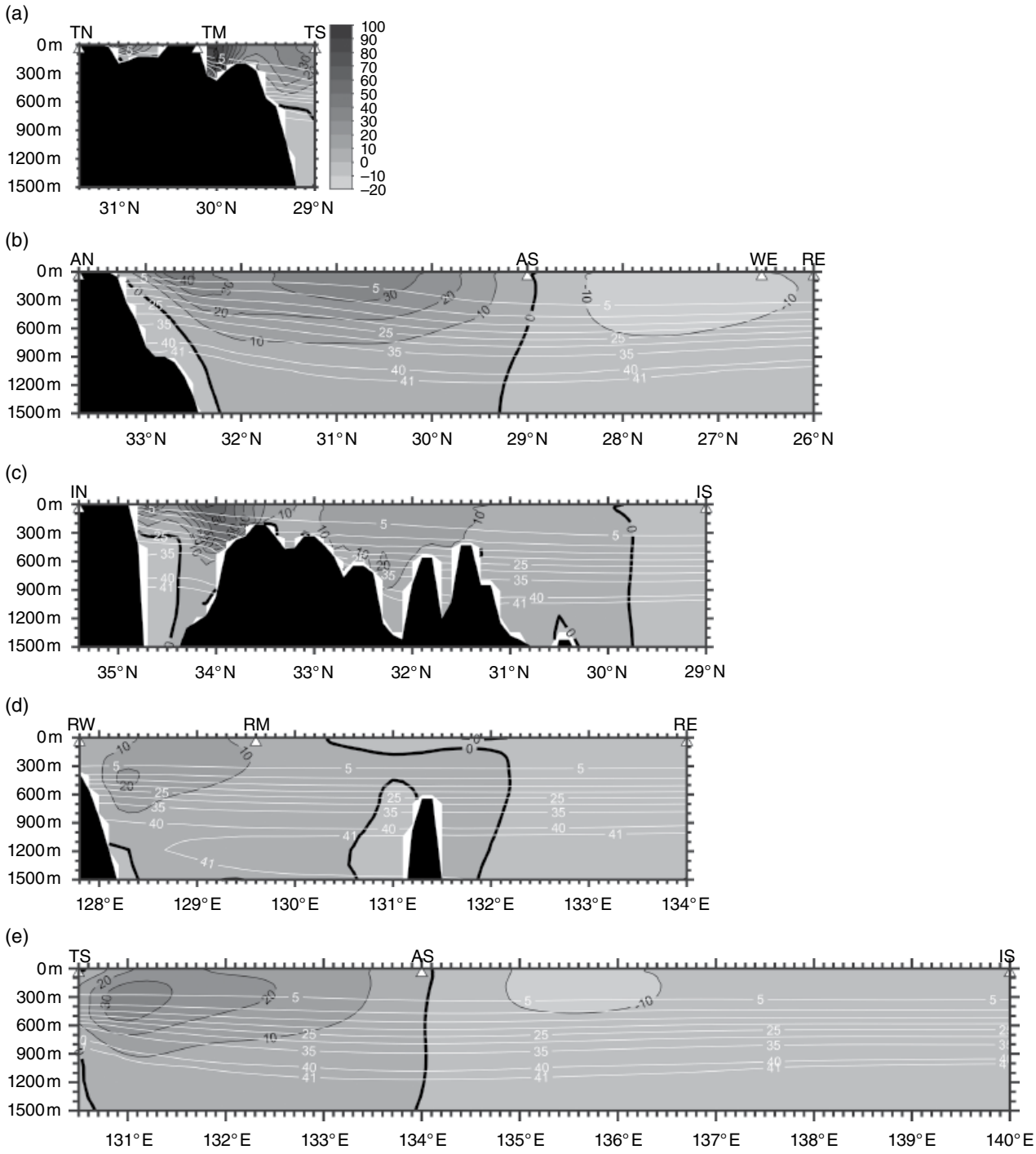

Figure 7.2 Temporally averaged current velocity (cm s^{-1}) normal to the sections and nitrate concentration (mmol m^{-3}) at each section. Color with black contours represents velocity with an interval of 10 cm s^{-1}. White contours indicate nitrate concentrations at intervals of 5 mmol m^{-3} with an exception of the maximum value of 41 mmol m^{-3}. Positive current velocity values are defined as having an eastward or northward direction, and thick black lines indicate a velocity of zero. Triangles at the top of the profiles denote endpoints and intermediate points of the sections shown in Figure 7.1.

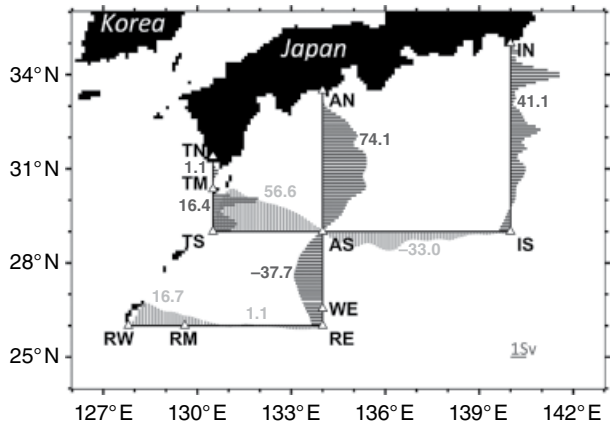

Figure 7.3 Volume transport (Sv) across the five sections. The length of dark gray (light gray) lines indicates volume transport across meridional (zonal) sections per horizontal distance of 0.1 degree. Dark gray (light gray) lines located at the right (upper) side of the section indicate an eastward (northward) volume transport. Numbers in dark gray (light gray) indicate total volume transport (Sv) through the section between adjacent triangles (e.g., 41.1 for section IN–IS). Positive values represent eastward or northward transport.

section AS–WE equal to the southward transport through section AS–IS (Figure 7.3). As will be shown in Section 7.4, the difference in nitrate transports between section AS–IS and section AS–WE will be treated as the contribution of Kuroshio recirculation to the nitrate transport south of Japan.

7.3.2. Vertical Profile of Nitrate Concentration and Nitrate Transport Through Sections

The nitrate concentration has a relatively simple distribution along the sections (dark gray lines in Figure 7.2), increasing with depth but showing slight variability in the horizontal direction. The nitrate concentration is less than 5 mmol m^{-3} in the upper layer (0–300 m), increases evenly to 40 mmol m^{-3} up to 900–1000 m, and keeps an almost constant value around 40 mmol m^{-3} below 900–1000 m (Figure 7.2).

The mean nitrate flux, defined as the product of monthly nitrate concentration and monthly current velocity and averaged over 1995– 2012, shows high variability in both the vertical and horizontal directions (Figure 7.4). A subsurface maximum core for eastward nitrate flux is found at three meridional sections and for the northward nitrate flux at two zonal sections. Subsurface maximum cores were also found for the westward nitrate flux at section AS–RE and for the southward nitrate flux at section AS–IS, both of which correspond to the Kuroshio recirculation south of Japan. At the Tokara Strait, a large flux is found in the bottom layer south of point TM (9 mmol m^{-2} s^{-1}) and the area over the shelf break (1 mmol m^{-2} s^{-1}) (Figure 7.4a), both of which have a relatively strong current (Figure 7.2a). In the area south of Japan, the eastward nitrate flux occupies a large area with a maximum value over 3 mmol m^{-2} s^{-1} at ~600 m depth, while the westward nitrate flux shows a maximum value over 2 mmol m^{-2} s^{-1} at ~800 m depth (Figure 7.4b). At the Izu-Ogasawara Ridge, the large eastward nitrate flux is concentrated mostly at the bottom layer with an exception at the surface layer near 35°N (Figure 7.4c). At section RW–RE, most of the area has a northward nitrate flux with a maximum value over 4 mmol m^{-2} s^{-1} near the shelf slope at 600 m depth (Figure 7.4d). Moving north, the northward nitrate flux increases markedly at section TS–AS where the northward nitrate flux at a depth of 600 m covers a larger area and has a larger maximum value (over 7 mmol m^{-2} s^{-1}) than at section RW–RE (Figure 7.4e). Meanwhile, the southward nitrate flux also appears at an area east of point AS with a maximum value over 1 mmol m^{-2} s^{-1} at a depth of ~800 m (Figure 7.4e).

Comparing the distributions of nitrate flux and current velocity at each of the sections, we find that the zero lines for the nitrate flux and current velocity do not always coincide with each other. This suggests that the average monthly nitrate flux does not always equal the product of mean current velocity and mean nitrate concentration. In other words, the product of the temporally variable components in nitrate concentration and current velocity also contribute to the mean nitrate flux through each section.

Similar to volume transport, we also present the horizontal distribution of nitrate transport through each grid point integrated from sea bottom to sea surface along the sections (Figure 7.5). At the Tokara Strait, the total eastward nitrate transport is 103.0 kmol s^{-1}, of which 99.4 kmol s^{-1} is attributed to section TM–TS. Eastward nitrate transport through section AN–AS is 979.7 kmol s^{-1}, most of which is distributed around the middle region of the section. Eastward nitrate transport at the Izu-Ogasawara Ridge decreases to 460.9 kmol s^{-1} and is characterized by several peak values along section IN–IS. Northward nitrate transport is 219.8 kmol s^{-1} at section RW–RM and 26.3 kmol s^{-1} at section RM–RE. The westward shift of northward nitrate transport at section RW–RE is also found at section TS–AS, where nitrate transport totaling 868.3 kmol s^{-1} is obtained. Meanwhile, southward nitrate transport is also found at section AS–IS where nitrate transport totals 514.0 kmol s^{-1} (Figure 7.5).

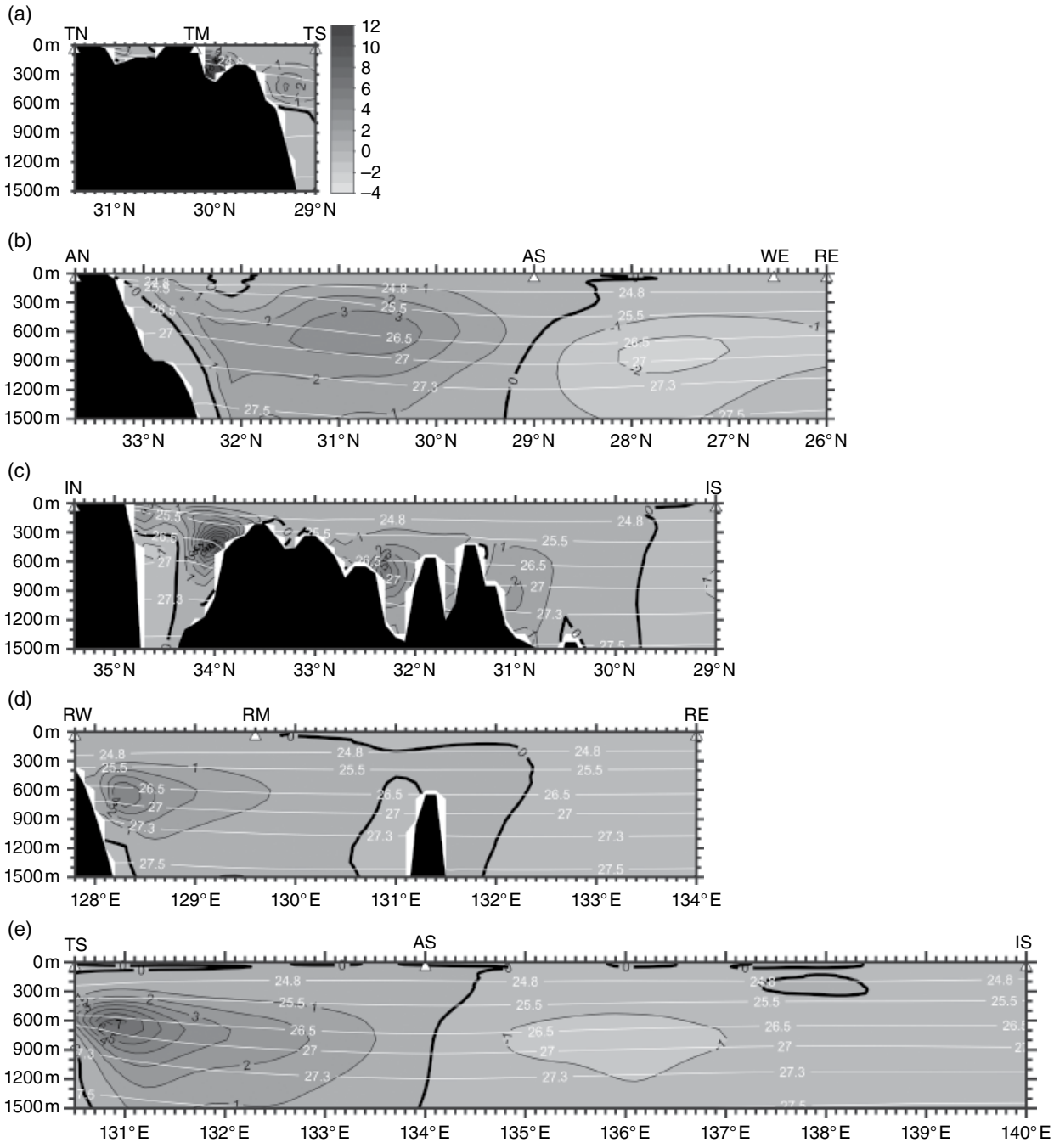

Figure 7.4 Temporally averaged nitrate flux (mmol m^{-2} s^{-1}) and potential density (σ_θ) for the sections. Color with black contours represent nitrate flux with an interval of 1 mmol m^{-2} s^{-1} and white contours show isopycnals of 24.80, 25.50, 26.50, 27.00, 27.30, 27.50 σ_θ. Positive nitrate flux values are defined as having an eastward or northward direction, and the thick black lines indicate zero flux. The upper triangles are the same as those in Figure 7.2. (*See insert for color representation of this figure.*)

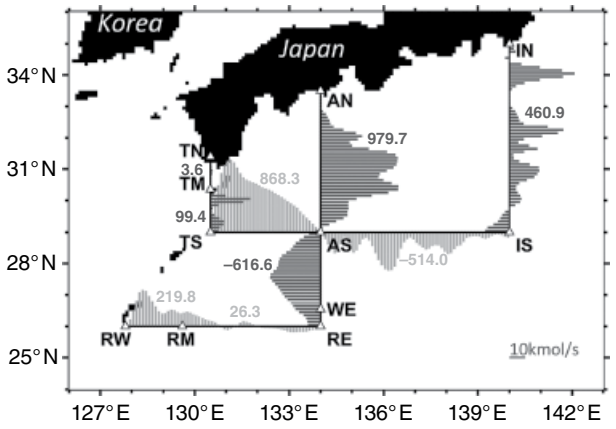

Figure 7.5 Nitrate transport (kmol s^{-1}) across the five sections. The length of dark gray (light gray) lines indicates nitrate transport across meridional (zonal) sections per horizontal distance of 0.1 degree. Dark gray (light gray) lines located at the right (upper) side of the section indicate an eastward (northward) nitrate transport. Numbers in dark gray (light gray) indicate total nitrate transport (kmol s^{-1}) through the section between adjacent triangles (e.g., 460.9 for section IN–IS). Positive values represent eastward or northward transport.

7.4. CONTRIBUTION OF RECIRCULATION TO VARIATION IN NUTRIENT TRANSPORT ALONG THE KUROSHIO PATH SOUTH OF JAPAN

There is an apparent increase in nitrate transport from the Tokara Strait (103.0 kmol s^{-1}) to south of Japan (979.7 kmol s^{-1} at section AN–AS). This increase is apparently caused by the contribution of northward nitrate transport across section TS–AS. The northward nitrate transport across section TS–AS has two components: one is the northeastward current east of the Ryukyu Islands that provides more than 246 kmol s^{-1} of nitrate transport to the Kuroshio south of Japan, and the other is the Kuroshio recirculation passing through sections AS–IS or AS–RE that contribute more than 600 kmol s^{-1} of nitrate transport to the Kuroshio south of Japan. Therefore, it is apparent that the Kuroshio recirculation contributes to the eastward nitrate transport south of Japan, which corroborates the conclusion of Guo et al. (2013).

On the other hand, there is also an apparent decrease in nitrate transport from the south of Japan (979.7 kmol s^{-1} at section AN–AS) to the Izu-Ogasawara Ridge (460.9 kmol s^{-1} at section IN–IS). This reduction is balanced by the southward nitrate transport through section AS–IS. The departure of the Kuroshio recirculation from the Kuroshio main stream is likely to cause the reduction of eastward nitrate transport from the south of Japan to the Izu-Ogasawara Ridge.

Taken together, the increase in eastward nitrate transport with the Kuroshio south of Japan from its entrance (Tokara Strait) to its exit (Izu-Ogasawara Ridge) is in the order of ~350 kmol s^{-1}. The northeastward current east of the Ryukyu Islands contributes to nitrate transport on the order of 245 kmol s^{-1}. This residual is generally balanced by the difference (~100 kmol s^{-1}) between southward nitrate transport across section AS–IS and westward nitrate transport at section AS–RE. The exact balance in the volume transport (Figure 7.3) but not in the nitrate transport among the sections (Figure 7.5) can be explained by variation in nitrate concentration among the sections (Guo et al., 2013).

If we consider that the Kuroshio recirculation has the same input and output of volume transport as it joins and leaves the Kuroshio main stream, its contribution to nitrate transport along the Kuroshio main stream is determined by the difference in nitrate concentration within the input water from the Kuroshio recirculation to the Kuroshio main stream and that within the output water from the Kuroshio main stream to the Kuroshio recirculation. The westward current through section AS–RE (input water) has a mean nitrate concentration of 16.35 mmol m^{-3} while the southward current through section AS–IS (output water) has a mean nitrate concentration of 15.58 mmol m^{-3}. Taking the difference (0.77 mmol m^{-3}) and the southward volume transport of 33.0 Sv through section AS–IS, the Kuroshio recirculation contributes 24.1 kmol s^{-1} to nitrate transport along the Kuroshio main stream. This value, however, is the contribution of mean current and mean nitrate concentration. The contribution of temporally variable components in current velocity and nitrate concentration to the mean nitrate transport should be also considered.

As defined in the last paragraph of section 7.3.1, we identify a point WE at section AS–RE where the volume transport through section AS–WE equals to that through section AS–IS. The westward mean nitrate transport through section AS–WE, as averaged from monthly values, is 559 kmol s^{-1} that is larger than the southward mean nitrate transport through section AS–IS by 45 kmol s^{-1}. Therefore, the contribution of Kuroshio recirculation to the mean nitrate transport along the Kuroshio main stream is 45 kmol s^{-1}, to which the mean current contributes 24.1 kmol s^{-1} while the temporally variable components contributes 20.9 kmol s^{-1}.

The large temporal variation in the volume transport through each section can be confirmed in Table 7.1. The detailed processes responsible for such large temporal variations in the volume transport and nitrate transport will be reported in another work. Another issue is the transport of biogenic particles including phytoplankton, zooplankton, and detritus. Because these biogenic particles are limited in the upper ocean and its concentration is also not high, their transports are smaller than the nitrate transport through the same section by 1–2 orders (Table 7.1).

Table 7.1 Mean and Standard Deviation of Transport for Water, Nitrate, Phytoplankton, Detritus and Zooplankton Through the Sections Shown in Figure 7.1. Northward and Eastward Transports are Defined as Positive Values.

Sections	Volume transport (Sv)	Nitrate transport (kmol s^{-1})	Phytoplankton transport (kmol s^{-1})	Detritus transport (kmol s^{-1})	Zooplankton transport (kmol s^{-1})
TM–TS	16.4 ± 3.4	99.4 ± 39.6	1.8 ± 0.6	1.6 ± 0.7	1.2 ± 0.5
TN–TM	1.1 ± 0.4	3.6 ± 2.0	0.3 ± 0.1	0.2 ± 0.1	0.2 ± 0.1
AN–AS	74.1 ± 40.0	979.7 ± 645.8	3.7 ± 1.9	2.8 ± 1.8	2.0 ± 1.1
AS–RE	−37.7 ± 47.7	−616.7 ± 752.2	−0.9 ± 2.0	−0.3 ± 1.7	−0.2 ± 1.1
IN–IS	41.1 ± 9.4	460.9 ± 165.4	3.1 ± 0.9	2.8 ± 1.1	2.0 ± 0.7
TS–AS	56.6 ± 38.2	868.3 ± 627.0	1.3 ± 1.6	0.7 ± 1.3	0.5 ± 0.8
AS–IS	−33.0 ± 40.0	−514.0 ± 625.9	−1.0 ± 1.7	−0.3 ± 1.5	−0.3 ± 0.9
RW–RM	16.7 ± 17.8	219.8 ± 358.7	0.4 ± 0.6	0.3 ± 0.4	0.2 ± 0.3
RM–RE	1.1 ± 23.8	26.3 ± 452.0	−0.1 ± 0.7	−0.1 ± 0.5	−0.1 ± 0.3

7.5. SUMMARY

Using monthly averaged output of an NPZD type model over the period 1995– 2012, we estimated the volume and nitrate transports around the Kuroshio south of Japan. There was an increase in nitrate transport of ~350 kmol s^{-1} from the Tokara Strait to the Izu-Ogasawa Ridge. Joining of the northeastward current east of the Ryukyu Islands with the Kuroshio is the main reason for the increase in nitrate transport over the entire area south of Japan. The Kuroshio recirculation contributes only in the order of 45 kmol s^{-1} to the increase in nitrate transport.

ACKNOWLEDGMENT

This study was supported by Grants-in-Aid for Scientific Research (MEXT KAKENHI grant numbers: JP15H05821/26287116). Y. Hu thanks the China Scholarship Council (CSC) for supporting her stay in Japan.

REFERENCES

Antonov, J. I., D. Seidov, T. P. Boyer, R. A. Locarnini, A. V. Mishonov, et al. (2010), *World Ocean Atlas 2009, Volume 2: Salinity*, U.S. Government Printing Office, Washington, DC.

Chen, C. C., Jan, S., Kuo, T. H., & Li, S. Y. (2017), Nutrient flux and transport by the Kuroshio east of Taiwan. *Journal of Marine System*, *167*, 43–54. https://doi.org/10.1016/j.jmarsys.2016.11.004.

Chen, C. T. A., Liu, C. T., & Pai, S. C. (1994), Transport of oxygen, nutrients and carbonates, by the Kuroshio current. *Chinese Journal of Oceanology and Limnology*, *12*(3), 220–227.

Chen, C. T. A., Liu, C. T., & Pai, S.C. (1995), Variations in oxygen, nutrient and carbonate fluxes of the Kuroshio Current. *La mer*, *33*, 161–176.

Guo, X., Zhu, X.-H., Wu, Q.-S., & Huang, D. (2012), The Kuroshio nutrient stream and its temporal variation in the East China Sea. *Journal of Geophysical Research*, *117*, C01026, doi: 10.1029/2011JC007292.

Guo, X., Zhu, X.-H., Long, Y., & Huang, D. (2013), Spatial variations in the Kuroshio nutrient transport from the East China Sea to south of Japan. *Biogeosciences*, *10*(10), 6403–6417, https://doi.org/10.5194/bg-10-6403-2013.

Imawaki, S., Uchida, H., Ichikawa, H., Fukasawa, M., Umatani, S. I., & the ASUKA Group. (2001), Satellite altimeter monitoring the Kuroshio transport South of Japan. *Geophysical Research Letters*, *28*(1), 17–20. https://doi.org/10.1029/2000GL011796.

Komori, N., Takahashi, K., Komine, K., Motoi, T., Zhang, X., & Sagawa, G. (2005), Description of sea-ice compartment of coupled ocean-sea-ice model for the Earth Simulator (OIFES). *Journal of Earth Simulator*, *4*, 31–45.

Locarnini, R. A., A. V. Mishonov, J. I. Antonov, T. P. Boyer, H. E. Garcia, O. K. Baranova, et al. (2010), *World Ocean Atlas 2009, Volume 1: Temperature*, U.S. Government Printing Office, Washington, DC.

Masumoto, Y., Sasaki, H., Kagimoto, T., Komori, N., Ishida, A., Sasai, Y., et al. (2004), A fifty-year-eddy-resolving simulation of the world ocean: preliminary outcomes of OFES (OGCM for the Earth Simulator). *Journal of Earth Simulator*, *1*, 35–56.

Nagano, A., Ichikawa, K., Ichikawa, H., Konda, M., & Murakami, K. (2013), Volume transports proceeding to the Kuroshio Extension region and recirculating in the Shikoku Basin. *Journal of Oceanography*, *69*(3), 285–293. https://doi.org/10.1007/s10872-013-0173-9.

Onogi, K., Tsutsui, J., Koide, H., Sakamoto, M., Kobayashi, S., Hatsushika, H., et al. (2007), The JRA-25 Reanalysis. *Journal of the Meteorological Society of Japan*, *85*, 369–432.

Oschlies, A. (2001), Model-derived estimates of new production: New results point towards lower values. *Deep Sea Research Part II: Topical Studies in Oceanography*, *48*, 2173–97.

Sasai, Y., Ishida, A., Sasaki, H., Kawahara, S., Uehara, H., & Yamanaka, Y. (2006), A global eddy-resolving coupled physical-biological model: physical influences on a marine ecosystem in the North Pacific. *Simulation-Transactions of the Society for Modeling and Simulation International*, *82*(7), 467–474, https://doi.org/10.1177/0037549706068943.

Sasai, Y., Richards, K.J., Ishida, A., & Sasaki, H. (2010), Effects of cyclonic mesoscale eddies on the marine ecosystem in the

Kuroshio Extension region using an eddy-resolving coupled physical-biological model. *Ocean Dynamics*, *60*, 693–704. https://doi.org/10.1007/s10236-010-0264-8.

Sasaki, H., M. Nonaka, Y. Masumoto, Y. Sasai, H. Uehara, & H. Sakuma (2008), An eddy-resolving hindcast simulation of the quasiglobal ocean from 1950 to 2003 on the Earth Simulator. In K. Hamilton & W. Ohfuchi (Eds.), *High Resolution Numerical Modelling of the Atmosphere and Ocean (157–185)*, Springer, New York.

Sugimoto, S., Hanawa, K., Narikiyo, K., Fujimori, M., & Suga, T. (2010), Temporal variations of the net Kuroshio transport and its relation to atmospheric variations. *Journal of Oceanography*, *66*(5), 611–619. https://doi.org/10.1007/s10872-010-0050-8.